Clinical Infectious Diseases

MAJOR ARTICLE

Antibody Banding Patterns of the Enzyme-Linked Immunoelectrotransfer Blot and Brain Imaging Findings in Patients With Neurocysticercosis

Gianfranco Arroyo,[1,2,3] Silvia Rodriguez,[4,a] Andres G. Lescano,[1,2,3] Karen A. Alroy,[5,b] Javier A. Bustos,[1,2,3,4] Saul Santivañez,[6] Isidro Gonzales,[4] Herbert Saavedra,[4] E. Javier Pretell,[7] Armando E. Gonzalez,[8] Robert H. Gilman,[5] Victor C. W. Tsang,[9] and Hector H. Garcia[1,2,3,4]; for the Cysticercosis Working Group in Peru[c]

[1]School of Public Health and Management, [2]Department of Microbiology, School of Sciences, and [3]Center for Global Health–Tumbes, Universidad Peruana Cayetano Heredia, and [4]Cysticercosis Unit, Instituto Nacional de Ciencias Neurológicas, Lima, Peru; [5]Department of International Health, Bloomberg School of Public Health, Johns Hopkins University, Baltimore, Maryland; [6]Instituto Peruano de Parasitología Clínica y Experimental, Lima, [7]Department of Neurology, Hospital Alberto Sabogal, Callao, and [8]School of Veterinary Medicine, Universidad Nacional Mayor de San Marcos, Lima, Peru; and [9]Georgia State University, Atlanta

Background. The enzyme-linked immunoelectrotransfer blot (EITB) assay is the reference serological test for neurocysticercosis (NCC). A positive result on EITB does not always correlate with the presence of active infections in the central nervous system (CNS), and patients with a single viable brain cyst may be EITB negative. Nonetheless, EITB antibody banding patterns appears to be related with the expression of 3 protein families of *Taenia solium*, and in turn with the characteristics of NCC in the CNS (type, stage, and burden of viable cysts).

Methods. We evaluated EITB antibody banding patterns and brain imaging findings of 548 NCC cases. Similar banding patterns were grouped into homogeneous classes using latent class analysis. The association between classes and brain imaging findings was assessed.

Results. Four classes were identified. Class 1 (patients negative or only positive to the GP50 band, related to the protein family of the same name) was associated with nonviable or single viable parenchymal cysticerci; class 2 (patients positive to bands GP42–39 and GP24, related to the T24-42 protein family, with or without anti-GP50 antibodies) was associated with intraparenchymal viable and nonviable infections; classes 3 and 4 (positive to GP50, GP42-39, and GP24 but also responding to low molecular weight bands GP21, GP18, GP14, and GP13, related to the 8 kDa protein family) were associated with extraparenchymal and intraparenchymal multiple viable cysticerci.

Conclusions. EITB antibody banding patterns correlate with brain imaging findings and complement imaging information for the diagnosis of NCC and for staging NCC patients.

Keywords. EITB; neurocysticercosis; *Taenia solium*; epilepsy; Peru.

Neurocysticercosis (NCC) is a zoonosis of the human central nervous system (CNS) caused by the cysticercus of the pork tapeworm *Taenia solium*, and is the leading cause of late-onset epilepsy worldwide [1–4]. Diagnosis of NCC is difficult. It depends on clinical and epidemiological criteria, supported by findings from neurologic imaging and serologic confirmation [5, 6]. Imaging constitutes the main diagnostic tool for physicians, allowing the recognition of cysticerci lodged in the brain, their type, stage, and number [3, 7, 8]. Magnetic resonance imaging (MRI) is more sensitive for diagnosing viable parenchymal and extraparenchymal NCC, whereas computed tomography (CT) is superior in detecting calcified lesions [7]. Imaging diagnosis is not always definitive. In some cases, images alone cannot differentiate NCC from other CNS lesions, and some NCC lesions may be missed on brain CT or MRI [9, 10].

The enzyme-linked immunoelectrotransfer blot assay using lentil-lectin purified glycoprotein parasite antigens (LLGP-EITB) is the best available serological test for NCC [11]. In this assay, specific antibody bands reacting against 7 defined *T. solium* antigens (GP50, GP42-39, GP24, GP21, GP18, GP14, and GP13, named by their molecular weight in kilodaltons [kDa]) are visually read, with high levels of specificity and sensitivity in patients with ≥2 viable brain cysts [11, 12]. Additionally, by detecting antibodies the EITB demonstrates evidence of exposure but not necessarily active infection. While the sensitivity of EITB is extremely high in patients with multiple viable lesions or extraparenchymal NCC, patients with a single brain lesion may have antibody responses not detectable by EITB and the antibody response may wane in patients with nonviable infections in the CNS, reducing the diagnostic capability of the EITB [13–15].

Received 7 June 2017; editorial decision 10 August 2017; accepted 29 August 2017; published online September 4, 2017.

[a]Deceased.

[b]Present affiliation: Centers for Disease Control and Prevention, Atlanta, Georgia.

[c]Members of the Cysticercosis Working Group in Peru are listed after the References.

Correspondence: H. H. Garcia, Department of Microbiology, Universidad Peruana Cayetano Heredia, Av. Honorio, Delgado 430, SMP, Lima 31, Peru (hgarcia1@jhu.edu).

Clinical Infectious Diseases® 2018;66(2):282–8

DOI: 10.1093/cid/cix774

In patients with symptomatic NCC looking for neurological care, EITB is usually a confirmatory tool supporting brain imaging findings for the diagnosis and follow-up of NCC patients [16, 17]. Additionally, the number of EITB antibody bands seen in clinical patients is greater than that observed in the general population [18, 19]. Nonetheless, the heterogeneity of EITB responses (expressed as antibody banding patterns) observed in clinical patients has not been studied in detail, nor how these banding patterns are related with the characteristics of NCC infection.

During the course of infection in the intermediate host, different sets of antigens of the *T. solium* cysticercus are expressed. These antigens demonstrate structural and functional differences and group into 3 protein families named as GP50 (comprised by the GP50 band alone), the T24-42 family (comprising the GP42-39 and GP24 bands) and the 8 kDa family (comprising the low molecular weight bands GP21, GP18, GP14, GP13, and eventually also found at the level of the GP24 band) [20–23]. The patterns of EITB antibody bands in clinical patients with NCC are not random [23], suggesting that their expression reflect the characteristics of the NCC in the host's CNS. We evaluated the relationship between EITB banding patterns with brain imaging findings of patients with NCC to demonstrate that the interpretation of their antibody banding patterns may supplement diagnostic imaging of NCC and contribute to its proper diagnosis.

MATERIALS AND METHODS

Samples and Study Design

Information regarding serological and brain image (CT and/or MRI) results, age, and sex from individuals with symptomatic NCC presenting for the first time to the Cysticercosis Unit at the Instituto Nacional de Ciencias Neurológicas in Lima, Peru, during a 6-year period (2009–2015) were retrieved from our archives. Potential study subjects were selected if they had a NCC diagnosis based on brain images, regardless of their EITB results. Individuals with negative neuroimages were not included. Cases where the nearest serum sample was taken >90 days before or after an index brain image (the initial image in record for each patient) were also excluded to avoid the effects of disease evolution or treatment measures.

Enzyme-Linked Immunoelectrotransfer Blot Assay

The LLGP-EITB assay was performed as described by Tsang et al [11]. In brief, 7 glycoprotein antigens of the *T. solium* cysticercus (GP50, GP42-49, GP24, GP21, GP18, GP14, and GP13), obtained by separation and purification using sodium dodecyl sulphate–polyacrylamide gel electrophoresis, were transferred from the gels to nitrocellulose membranes and incubated in duplicate with pretreated serum samples, using 3.3′diaminobenzimidine tetrahydrochloride dihydrate as substrate for the visualization of bands (color development). Banding pattern readings were performed in 2 steps (a first reading is performed by the laboratory technician performing the assays, and then all results are revised by a supervisor. All dubious responses are selected for reprocessing, as well as a random 5% of all processed samples). Readers are blinded from imaging results to prevent any biases. The presence or absence of each of the 7 bands was recorded and coded to create the variable "EITB banding pattern," as a chain of 7 consecutive 0 and 1 values indicating the absence or presence of each of the bands, respectively.

Images

Image readings were performed by a neuroradiologist external to the study and confirmed by neurologists on the study team. Radiological data (type, stage, and number of cysticerci) were collected. Extraparenchymal NCC was defined as the presence of ventricular and/or subarachnoid cysticerci. Intraparenchymal NCC was defined as the presence of live, viable, and/or degenerated cysticerci, with or without calcifications into the brain parenchyma. For the analyses, extraparenchymal NCC was the defining characteristic based on its strong serological response, thus mixed intra- and extraparenchymal infections were allocated into the extraparenchymal subgroup. Similarly, the presence of at least 1 live, viable cysticercus (with or without nonviable infection) classified the case as viable NCC. The number of live viable cysticerci was also recorded. Degenerated cysts and/or calcified lesions met criteria to be included in the nonviable subgroup.

Statistical Analysis

NCC patient characteristics were summarized using descriptive statistics. We performed a latent class analysis using the results of each of the 7 EITB bands (observed variables) to group banding patterns in homogeneous classes that represent different characteristics of CNS infection, in terms of the type, stage, and number of cysts (latent variable). Patients with unusual banding patterns (each representing <1% of the observed banding patterns in the study subjects) were excluded from the analysis to avoid their inclusion in classes as residuals. Five models with increasing numbers of classes (2–6) were fitted by maximum likelihood processes [24]. The optimal number of classes was established according to a statistical criterion (the model with the smallest Bayesian information criterion to account for model fit and parsimony [24]) and interpretability of classes (distribution of representative banding patterns in each class). Once the optimal number of classes was established, 2 model parameters (class prevalences approximately ≥10% among classes and probabilities of bands conditional to class membership close to 0 or 1) were evaluated to confirm model structure [24]. Model stability was confirmed by random split-half reanalysis of the data (with and without patients with unusual banding patterns).

Bivariate associations between classes and age, sex, and imaging findings were performed using χ^2 and Kruskal-Wallis tests as required. The relationship between banding pattern classes (outcome variable) and brain imaging findings was assessed using multinomial logistic regression analyses. Three separate models for cyst type, cyst stage, and cyst burden (each adjusted by age and sex) were fitted and odds ratios (ORs) with 95% confidence intervals (CIs) for the presence of banding pattern classes were calculated. Statistical analyses were performed in R version 3.3.1, using the package poLCA for latent class analysis. *P* values < .05 were considered significant.

Ethical Considerations

This study was previously approved by the Institutional Review Board (IRB) of the Universidad Peruana Cayetano Heredia (approval number: 0006689). Anonymized archive sera samples and brain image information were evaluated, collected in prior IRB-approved studies with written informed consents specifically allowing future use of the collected samples.

RESULTS

There were 548 eligible cases during the study period. Subjects had a mean age of 45 ± 16.8 years, and 56% were women (305/548). Four hundred individuals (73%) had intraparenchymal NCC and 220 (55%) of them had at least 1 viable cysticerci only (median, 2 [range, 1–102]), while 180 (45%) had nonviable cysticerci only, many of them calcified cysts (172/180 [96%]), and less frequently granulomas with or without calcifications (8/180 [4%]) (Figure 1). One hundred forty-eight individuals (27%) had extraparenchymal NCC, 120 of them (81%) harboring subarachnoid cysts; 18 (12%) had ventricular cysts, and 10 (7%) had both type of cysts. The median number of EITB bands was 5 (range, 0–7). Most cases reacted positively to the EITB bands of high molecular weight (85.2%, 86.3%, and 84.3% for bands GP50, GP42-39, and GP24, respectively) compared to the reaction against the low molecular weight bands (49.8%, 47.1%, 50.7%, and 55.5% for bands GP21, GP18, GP14, and GP13 respectively) (Figure 2); 56 (10%) of NCC cases were EITB-negative, all being cases with intraparenchymal infections, mostly nonviable (56 [93%]) or with single viable cysts only (4 [7%]).

Sixteen (3%) of the study subjects had unusual banding patterns and were excluded from latent class analysis. A 4-class model was considered the optimal according to its smallest Bayesian information criterion compared with models of 2, 3, 5, and 6 classes (Supplementary Table 1). Representative banding patterns were also observed in each class (Table 1). Class 1 (n = 75) included primarily patients EITB-negative (75%) or positive to the GP50 only, corresponding to the protein family of the same name. Class 2 (n = 142) included patients positive to bands GP42-39 and GP24 (related to the T24-42 protein family) with or without GP50. Class 3 (n = 51) and class 4 (n = 264) included patients who were positive to the high molecular weight bands (GP50, GP42-39, and GP24) similar to class 2, but in addition were also positive to the low molecular weight bands related to the 8 kDa protein family (GP21, GP18, GP14, and GP13). Classes 3 and 4 were defined as "positive" and "strongly positive" to antigens of the 8 kDa protein family according to the number of low molecular weight bands seen in each class (GP14 and GP13 in class 3, and GP14, GP13 and additionally GP21 and GP18 in class 4). Class prevalences were higher in classes 4 and 2 (50% and 27%, respectively) compared with classes 1 and 3 (14% and 9%, respectively). Probabilities of bands conditional to class membership were >80% for bands GP50, GP42-39, and GP24 in classes 2, 3, and 4 and >90% for bands GP21, GP18, GP14, and GP13 in class 4; the smallest conditional probability was observed for GP50 conditional to membership in class 1 (Supplementary Table 2). Model stability was confirmed with reanalysis using half of the data randomly selected, and banding pattern classes did not change when analyses included the 16 patients with unusual banding patterns (data not shown).

Bivariate analyses showed a strong association between antibody banding pattern classes and brain imaging findings (all *P* < .001; Table 2). Extraparenchymal NCC cases were more frequent in classes 4 (119/264 [45%]) and 3 (16/51 [31%]); NCC cases with intraparenchymal viable cysticerci were also more frequent in classes 3 (28/35 [80%]) and 4 (118/145 [81%]), and these classes had higher medians of viable cysts (median, 3 [range, 1–102] for class 4 and median, 3 [range, 1–99] for class 3). Cases with viable cysticerci in the class 2 had a median of 1 (range, 1–79), whereas viable infections in class 1 corresponded to single cysts only. Most cases of nonviable intraparenchymal

Table 1. Class Description and Distribution of Enzyme-Linked Immunoelectrotransfer Blot Antibody Banding Patterns in Each of the Classes (N = 532 Cases)

Class Description	EITB Antibody Banding Patterns[a]	No. (%)
Class 1 (negative or positive to antigens of the GP50 protein family)		n = 75
	0000000	56 (74.7)
	1000000	19 (25.3)
Class 2 (positive to antigens of the T24-42 protein family, with or without GP50)		n = 142
	0110000	22 (15.5)
	1100000	8 (5.6)
	1110000	112 (78.9)
Class 3 (positive to antigens of the GP50, T24-42, and 8 kDa protein families)		n = 51
	1110001	34 (67)
	1110011	17 (33)
Class 4 (positive to antigens of the GP50 and T24-42 protein family and strongly positive to antigens of the 8 kDa protein family		n = 264
	1111011	11 (4.2)
	1111100	7 (2.7)
	1111110	13 (4.9)
	1111111	233 (88.3)

Abbreviation: EITB, enzyme-linked immunoelectrotransfer blot.

[a]Values of 1 and 0 represent the presence or absence, respectively, of each of the EITB bands (GP50, GP42-39, GP24, GP21, GP18, GP14, and GP13)

Table 2. Distribution of Age, Sex, and Characteristics of the Central Nervous System Infection (Type, Stage, and Number of Cysticerci) According to Enzyme-Linked Immunoelectrotransfer Blot Banding Pattern Classes[a] in Neurocysticercosis Cases

Variables	Class 1 (n = 75)	Class 2 (n = 142)	Class 3 (n = 51)	Class 4 (n = 264)	*P* Value
Age, y[b]	41.2 ± 14.5	43.3 ± 16.8	48.4 ± 17.3	46.4 ± 16.9	.029
Sex					
Female	49 (65.3)	85 (59.9)	26 (51.0)	136 (51.5)	.105
Male	26 (34.7)	57 (40.1)	25 (49.0)	128 (48.5)	
Cyst type					
Intraparenchymal	75 (100.0)	131 (92.3)	35 (68.6)	145 (54.9)	<.001
Extraparenchymal	0 (0.0)	11 (7.7)	16 (31.4)	119 (45.1)	
Cyst stage[c]					
Nonviable	69 (92.0)	73 (55.7)	7 (20.0)	27 (18.6)	<.001
Viable	6 (8.0)	58 (44.3)	28 (80.0)	118 (81.4)	
Cyst burden[d], median (IQR)	1[e]	1 (2)	3 (3.5)	3 (9)	<.001

Data are presented as No. (%) unless otherwise indicated.

Abbreviation: IQR, interquartile range.

[a]Classes: 1 (negative or positive to antigens of the GP50 protein family); 2 (positive to antigens of the protein T24-42 protein family, with or without GP50); 3 (positive to antigens of the GP50, T24-42, and 8 kDa protein families); and 4 (positive to antigens of the GP50 and T24-42 protein families and strongly positive to antigens of the 8 kDa protein family).

[b]Mean ± standard deviation.

[c]Evaluated in intraparenchymal neurocysticercosis (NCC) cases only.

[d]Evaluated in intraparenchymal NCC cases with viable cysts only.

[e]Single viable cysts only were observed.

infections were observed in classes 1 (69/75 [92%]) and 2 (73/131 [56%]). Distribution of banding pattern classes by age and sex showed older cases in classes 3 and 4 than those in classes 2 and 1 (P = .023), but there were no significant differences by sex. Extraparenchymal NCC cases were older than intraparenchymal NCC cases (P < .001); cases with nonviable and viable cysticerci were similar according to age, but different according to sex (67% of cases with nonviable infections were women; P = .001).

Associations between banding pattern classes and brain imaging findings remained strong after adjustment by age and sex in the regression models, suggesting that type, stage, and number of lesions are the major drivers for banding pattern classes (Table 3). Using class 2 as reference outcome, cases with extraparenchymal NCC and cases with viable intraparenchymal cysts had high odds of having banding patterns of classes 4 (ORs, 9.7 [95% CI, 4.9–19] and 5.4 [95% CI, 3.1–9.4]) or 3 (ORs, 4.9 [95% CI, 2.1–11.7] and 4.8 [95% CI, 1.9–11.8]); cases with nonviable intraparenchymal infections had high odds of being EITB negative or positive to GP50 only (class 1; OR, 9.2 [95% CI, 3.7–22.9]); cases with ≥2 viable cysts had significantly higher odds of having banding patterns of class 4 (OR, 3.2 [95% CI, 1.7–6.3]), whereas the odds of having banding patterns of class 3 was higher but not significant (OR, 2.4 [95% CI, .9–2.2]).

DISCUSSION

Our study shows that the distribution of antibody banding patterns on LLGP-EITB is related to the type and characteristics of human NCC (type, stage, and number of cysts). Banding pattern classes representative of strong (classes 3 and 4) or weak (classes 1 and 2) antibody responses are more common in some NCC forms than others, and stronger antibody responses include those to smaller molecular weight antigens. This information may help to optimize the use of serological information in the diagnosis and follow-up of NCC patients.

We identified 4 clearly differentiated but internally homogeneous banding pattern classes. The distribution of EITB banding patterns in these classes (GP50 alone in class 1, GP42-39 and GP24 with or without GP50 in class 2, and all of these plus GP14 and GP13 in class 3 or GP21, GP18, GP14, and GP13 in class 4) strongly correlates with the distribution of these antigens in the 3 known protein families [20–23]. Departing from reactions to the GP50 family in class 1, reactions to the T24-42 family add in class 2, and reactions to the antigens of the 8 kDa protein family are added in class 3 and class 4. Classes 3 and 4 include antibody responses to antigens of the same protein

Table 3. Multinomial Logistic Regression Models Adjusted by Age (in Deciles) and Sex for the Calculations of Odds Ratios for the Presence of Antibody Banding Pattern Classes[a] in Neurocysticercosis Cases According to Characteristics of the Central Nervous System Infection

	Class 1		Class 3		Class 4	
Characteristics of NCC in the CNS	AOR[b] (95% CI)	*P* Value	AOR[b] (95% CI)	*P* Value	AOR[b] (95% CI)	*P* Value
Cyst type						
Extraparenchymal vs intraparenchymal (reference)	…	…	4.9 (2.1–11.7)	<.001	9.7 (4.9–19.0)	<.001
Cyst stage[c]						
Viable vs nonviable (reference)	0.1 (.0– 0.3)	<.001	4.8 (1.9–11.8)	.001	5.4 (3.1– 9.4)	<.001
Cyst burden[d]						
Two or more cysts vs single cysts (reference)	…	…	2.4 (.9– 6.2)	.068	3.2 (1.7– 6.3)	.001

Abbreviations: AOR, adjusted odds ratio; CI, confidence interval; CNS, central nervous system; NCC, neurocysticercosis.

[a]Class 1 (negative or positive to antigens of the GP50 protein family); class 2 (positive to antigens of the protein T24-42 protein family, with or without GP50); class 3 (positive to antigens of the GP50, T24-42, and 8 kDa protein families); class 4 (positive to antigens of the GP50 and T24-42 protein families and strongly positive to antigens of the 8 kDa protein family).

[b]For the calculation of odds ratios, class 2 was the reference outcome.

[c]Evaluated in intraparenchymal NCC cases only.

[d]Evaluated in intraparenchymal NCC cases with viable cysticerci only.

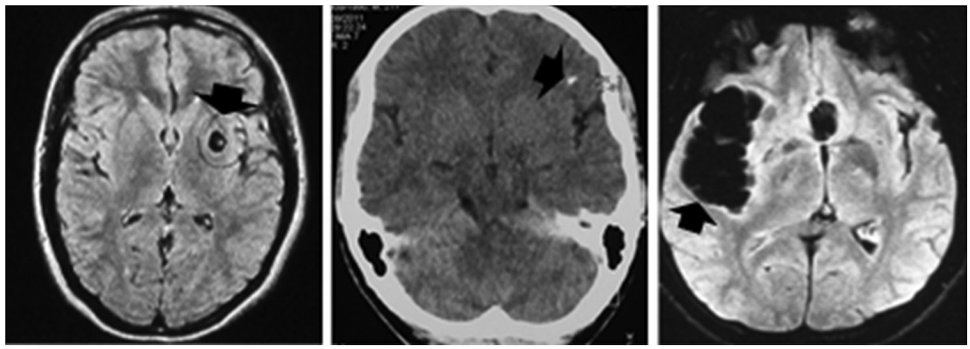

Figure 1. Characteristics of the central nervous system infection in neurocysticercosis. Left: Viable parenchymal brain cysts (magnetic resonance imaging [MRI], fluid attenuation inversion recovery [FLAIR] protocol). Center: Calcified parenchymal lesion (noncontrast computed tomography [black arrow]). Right: Subarachnoid extraparenchymal cysticercosis (MRI, FLAIR protocol).

family. Class 4 shows a stronger antibody response compared to class 3 (a greater number of low molecular weight antibody bands was seen in class 4). Additionally, the inclusion of classes 3 and 4 as separate classes improves the interpretability of the remaining classes in the model (not seen in the models with 2, 3, 5, and 6 classes).

Age and sex did not strongly influence antibody banding class membership according to imaging findings in our study. We would have expected an older age in individuals in class 1 due to already resolved infections. However, negative or GP50-only reactions could also result from early infections in individuals with a single cyst, and these could have lowered the mean age in this class. The group of older, resolved cases was likely underrepresented in our sample of individuals attending a referral center by the first time.

Class 1 (EITB negative or positive to GP50) was related with nonviable infections or cases with a single viable intraparenchymal cysticercus. In this class, individuals positive to single band GP50 were similar to those EITB negative in terms of brain imaging findings. A few cases of apparent false positive reactions to GP50 have been also reported in the literature [25, 26]. Our data suggest that GP50 alone in the absence of other diagnostic bands is rarely associated with established infections with multiple cysts or extraparenchymal NCC.

Class 2 (positive to antigens of the T24-42 protein family with or without GP50) had combinations of the high molecular weight bands (GP50, GP42-39, and GP24), recognized as the most immunodominant in the EITB [11, 27, 28]. Antigens of the T24-42 family are recognized as tetraspanins [22], membrane proteins involved in processes of cell proliferation, adhesion, motility, and scaffolding for the assembly of various complexes of proteins at the cell membrane [22, 29]. Due to their immunodominance, these banding patterns may persist in patients with nonviable NCC as observed in our study. Some patients in class 2 (corresponding to combinations of GP50, GP42-39, and GP24) had high-burden intraparenchymal infections as well as extraparenchymal infections, expected to express antigens from the 8 kDa protein family. As described by Hancock et al [22], while most 8 kDa antigens migrate at the low molecular weight bands, some remain at the level of the GP24 band (belonging to class 2 in our analysis).

Classes 3 and 4 were strongly associated with extraparenchymal NCC as well as with intraparenchymal viable infections with a high cyst burden. Antigens belonging to the 8 kDa protein family (distributed in the bands GP21, GP18, GP14, and GP13 seen in classes 3 and 4) have been classified as excretory/secretory proteins associated with evasive immune responses [23, 30]. The presence of these bands has also been associated with a higher probability of viable cysticerci in the brain parenchyma in previous studies [11, 18]. Classes 3 and 4 are similar in structure, but they differ in the number of reactive low molecular weight antibody bands (stronger antibody responses to antigens of the 8 kDa protein family for class 4 compared with class 3).

Our study had some limitations to consider. Due to the cross-sectional design, we cannot differentiate if the imaging findings on banding pattern classes corresponded to new or chronic infections. The exclusion of patients with no evidence of NCC on brain imaging limits our assessment to cases where lesions were apparent in neuroimaging and perhaps results in selection bias toward more evident infections. Data on prior antiparasitic treatment of patients were not available. Even when we only included the EITB results in sera of patients taken within 90 days before or after their initial brain image, it is possible that some patients had received antiparasitic therapy before attending our unit for first time and, as such, potential bias is possible due to the lack of control for this variable.

Additionally, the lack of covariates of clinical relevance (length of illness, symptoms, etc), could have resulted in a non-controlled confounding effect. Nonetheless, clinical symptoms do not play too much of a role here, since calcified or degenerating cysts can be highly symptomatic in NCC cases, irrespective of the presence of viable cysts or antibody responses. Finally, the EITB provides a qualitative rather than a quantitative result, so further studies using quantitative methods, such

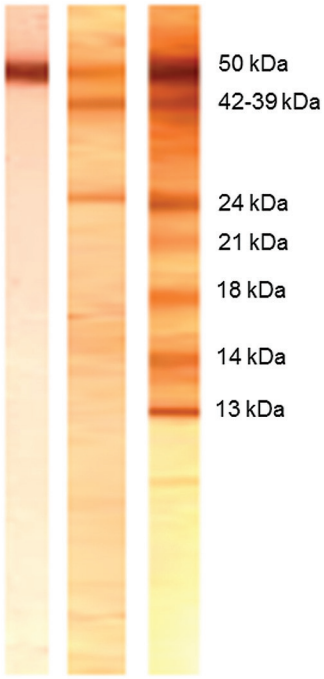

Figure 2. Antibody banding patterns of the lentil-lectin glycoprotein enzyme-linked immunoelectrotransfer blot (EITB) assay. Banding patterns of patients positive to GP50 only (left), GP50 plus GP42-39 and GP24 (center), and positive to all 7 antibody bands (right). Respective molecular weights for each of the EITB bands are also shown.

as enzyme-linked immunosorbent assay and/or Luminex, could unveil other associations not detected here.

EITB banding patterns match quite well the heterogeneity of NCC brain imaging findings. Banding patterns of classes 3 and 4 (antibody responses to antigens of the 8 kDa protein family) are observed in highly antigenic infections (extraparenchymal NCC and intraparenchymal NCC with high cyst burden), whereas banding patterns of class 2 (antibody responses to antigens of the T24-42 protein family) are mostly observed in nonviable and viable intraparenchymal infections. Banding patterns of class 1 (negative or positive to the GP50 protein family) usually have intraparenchymal nonviable NCC or single viable cysticerci. The interpretation of the EITB banding patterns should provide valuable information for the diagnosis, characterization, and follow-up of NCC cases.

Supplementary Data

Supplementary materials are available at *Clinical Infectious Diseases* online. Consisting of data provided by the authors to benefit the reader, the posted materials are not copyedited and are the sole responsibility of the authors, so questions or comments should be addressed to the corresponding author.

Notes

Acknowledgments. The authors thank Erika Perez and Karen Arteaga at the Cysticercosis Unit, Instituto Nacional de Ciencias Neurológicas de Lima, for their hard work in processing and storing samples used in this study, and to the Centers for Disease Control and Prevention (CDC) staff (P. Wilkins, S. Handali, J. Noh) for continuous technical support. This article is dedicated to the memory of Dr Silvia Rodriguez in recognition of her contribution as laboratory chief of the Cysticercosis Unit in the standardization and implementation of the EITB as a routine test for serological diagnosis of NCC.

Disclaimer. The funders had no role in the study design, sample collection, analysis, interpretation, writing of the manuscript, or the decision to submit the article for publication. Contributions to this manuscript by Dr Karen A. Alroy were done in her personal capacity. The information presented does not necessarily reflect the view of the Centers for Disease Control and Prevention, the Department of Health and Human Services, or the United States government.

Financial support. This work was partially supported by the Fogarty International Center/NIH (training grant numbers D43TW001140 and D43TW007393) and by the National Council for Science, Technology and Innovation of Peru (CONCYTEC).

Potential conflicts of interest. All authors: No reported conflicts of interest. All authors have submitted the ICMJE Form for Disclosure of Potential Conflicts of Interest. Conflicts that the editors consider relevant to the content of the manuscript have been disclosed.

References

1. White AC Jr. Neurocysticercosis: a major cause of neurological disease worldwide. Clin Infect Dis **1997**; 24:101–13; quiz 114–5.
2. Rajshekhar V. Neurocysticercosis: diagnostic problems and current therapeutic strategies. Indian J Med Res **2016**; 144:319–26.
3. Garcia HH, Nash TE, Del Brutto OH. Clinical symptoms, diagnosis, and treatment of neurocysticercosis. Lancet Neurol **2014**; 13:1202–15.
4. Nash TE, Garcia HH. Diagnosis and treatment of neurocysticercosis. Nat Rev Neurol **2011**; 7:584–94.
5. Del Brutto OH, Rajshekhar V, White AC Jr, et al. Proposed diagnostic criteria for neurocysticercosis. Neurology **2001**; 57:177–83.
6. Del Brutto OH, Nash TE, White AC Jr, et al. Revised diagnostic criteria for neurocysticercosis. J Neurol Sci **2017**; 372:202–10.
7. García HH, Del Brutto OH. Imaging findings in neurocysticercosis. Acta Trop **2003**; 87:71–8.
8. Takayanagui OM, Odashima NS. Clinical aspects of neurocysticercosis. Parasitol Int **2006**; 55:S111–5.
9. Agapejev S. Neurocysticercosis: the enigmatic disease. Cent Nerv Syst Agents Med Chem **2011**; 11:261–84.
10. Zea-Vera A, Cordova EG, Rodriguez S, et al; Cysticercosis Working Group in Peru. Parasite antigen in serum predicts the presence of viable brain parasites in patients with apparently calcified cysticercosis only. Clin Infect Dis **2013**; 57:e154–9.
11. Tsang VC, Brand JA, Boyer AE. An enzyme-linked immunoelectrotransfer blot assay and glycoprotein antigens for diagnosing human cysticercosis (*Taenia solium*). J Infect Dis **1989**; 159:50–9.
12. Wilson M, Bryan RT, Fried JA, et al. Clinical evaluation of the cysticercosis enzyme-linked immunoelectrotransfer blot in patients with neurocysticercosis. J Infect Dis **1991**; 164:1007–9.
13. Garcia HH, Herrera G, Gilman RH, et al. Discrepancies between cerebral computed tomography and western blot in the diagnosis of neurocysticercosis. the Cysticercosis Working Group in Peru (Clinical Studies Coordination Board). Am J Trop Med Hyg **1994**; 50:152–7.
14. Garcia HH, Gilman RH, Catacora M, Verastegui M, Gonzalez AE, Tsang VC. Serologic evolution of neurocysticercosis patients after antiparasitic therapy. Cysticercosis Working Group in Peru. J Infect Dis **1997**; 175:486–9.
15. Garcia HH, Gonzalez AE, Gilman RH, et al; Cysticercosis Working Group in Peru. Short report: transient antibody response in *Taenia solium* infection in field conditions—a major contributor to high seroprevalence. Am J Trop Med Hyg **2001**; 65:31–2.
16. Garcia HH, Rodriguez S, Gilman RH, Gonzalez AE, Tsang VC; Cysticercosis Working Group in Peru. Neurocysticercosis: is serology useful in the absence of brain imaging? Trop Med Int Health **2012**; 17:1014–8.
17. Rodriguez S, Dorny P, Tsang VC, et al; Cysticercosis Working Group in Peru. Detection of *Taenia solium* antigens and anti–*T. solium* antibodies in paired serum and cerebrospinal fluid samples from patients with intraparenchymal or extraparenchymal neurocysticercosis. J Infect Dis **2009**; 199:1345–52.
18. Bern C, Garcia HH, Evans C, et al. Magnitude of the disease burden from neurocysticercosis in a developing country. Clin Infect Dis **1999**; 29:1203–9.
19. Gonzales I, Miranda JJ, Rodriguez S, et al; Cysticercosis Working Group in Peru. Seizures, cysticercosis and rural-to-urban migration: the PERU MIGRANT study. Trop Med Int Health **2015**; 20:546–52.
20. Hancock K, Pattabhi S, Greene RM, et al. Characterization and cloning of GP50, a *Taenia solium* antigen diagnostic for cysticercosis. Mol Biochem Parasitol **2004**; 133:115–24.

21. Hancock K, Pattabhi S, Whitfield FW, et al. Characterization and cloning of T24, a *Taenia solium* antigen diagnostic for cysticercosis. Mol Biochem Parasitol **2006**; 147:109–17.
22. Hancock K, Khan A, Williams FB, et al. Characterization of the 8-kilodalton antigens of *Taenia solium* metacestodes and evaluation of their use in an enzyme-linked immunosorbent assay for serodiagnosis. J Clin Microbiol **2003**; 41:2577–86.
23. Rodriguez S, Wilkins P, Dorny P. Immunological and molecular diagnosis of cysticercosis. Pathog Glob Health **2012**; 106:286–98.
24. Lanza ST, Rhoades BL. Latent class analysis: an alternative perspective on subgroup analysis in prevention and treatment. Prev Sci **2013**; 14:157–68.
25. Kojic EM, White AC Jr. A positive enzyme-linked immunoelectrotransfer blot assay result for a patient without evidence of cysticercosis. Clin Infect Dis **2003**; 36:e7–9.
26. Furrows SJ, McCroddan J, Bligh WJ, Chiodini P. Lack of specificity of a single positive 50-kDa band in the electroimmunotransfer blot (EITB) assay for cysticercosis. Clin Microbiol Infect **2006**; 12:459–62.
27. García HH, Gilman RH, Gonzalez AE, et al; Cysticercosis Working Group in Perú. Hyperendemic human and porcine *Taenia solium* infection in Perú. Am J Trop Med Hyg **2003**; 68:268–75.
28. Esquivel-Velázquez M, Ostoa-Saloma P, Morales-Montor J, Hernández-Bello R, Larralde C. Immunodiagnosis of neurocysticercosis: ways to focus on the challenge. J Biomed Biotechnol **2011**; 2011:516042.
29. Maecker HT, Todd SC, Levy S. The tetraspanin superfamily: molecular facilitators. FASEB J **1997**; 11:428–42.
30. Ferrer E, Bonay P, Foster-Cuevas M, et al. Molecular cloning and characterisation of Ts8B1, Ts8B2 and Ts8B3, three new members of the *Taenia solium* metacestode 8 kDa diagnostic antigen family. Mol Biochem Parasitol **2007**; 152:90–100.
31. Tuero I, Palma S, Cabeza F, et al. A comparative study of peripheral immune responses to *Taenia solium* in individuals with parenchymal and subarachnoid neurocysticercosis. PLoS Negl Trop Dis **2015**; 9:e0004143.

Cysticercosis Working Group in Peru

Hector H. Garcia, MD, PhD; Robert H. Gilman, MD, DTMH; Armando E. Gonzalez, DVM, PhD; and Victor C. W. Tsang, PhD (Coordination Board); Silvia Rodriguez, MSc; Isidro Gonzalez, MD; Herbert Saavedra, MD; Manuel Martinez, MD; Manuel Alvarado, MD (Instituto Nacional de Ciencias Neurológicas, Lima, Peru); Manuela Verastegui, PhD; Mirko Zimic, PhD; Javier Bustos, MD, MPH; Holger Mayta, PhD; Cristina Guerra, PhD; Yesenia Castillo, MSc; Yagahira Castro, MSc (Universidad Peruana Cayetano Heredia, Lima, Peru); Maria T. Lopez, DVM, PhD; Cesar M. Gavidia, DVM, PhD; Luis Gomez, DVM (School of Veterinary Medicine, Universidad Nacional Mayor de San Marcos, Lima, Peru); Luz M. Moyano, MD; Ricardo Gamboa, MSc; Claudio Muro; Percy Vilchez, MSc (Cysticercosis Elimination Program, Tumbes, Peru); Theodore E. Nash, MD; Siddhartha Mahanty, MD, PhD (National Institute for Allergy and Infectious Diseases, National Institutes of Health [NIH], Bethesda, Maryland); John Noh, BS, Sukwan Handali, MD (CDC, Atlanta, Georgia); Jon Friedland (Imperial College, London, United Kingdom).